Petra Mela[1]
Niels R. Tas[1]
Erwin J. W. Berenschot[2]
Jan van Nieuwkasteele[1]
Albert van den Berg[1]

[1]BIOS, MESA+ Institute for Nanotechnology
[2]Transducers Science and Technology, MESA+ Institute for Nanotechnology,
University of Twente,
Enschede, The Netherlands

Electrokinetic pumping and detection of low-volume flows in nanochannels

Electrokinetic pumping of low-volume rates was performed on-chip in channels of small cross sectional area and height in the sub-μm range. The flow was detected with the current monitoring technique by monitoring the change in resistance of the fluid in the channel upon the electroosmosis-driven displacement of an electrolyte solution by a second electrolyte solution. Flow rates in the order of 0.1 pL/s were successfully generated and detected. The channels were fabricated with the sacrificial layer technology.

Keywords: Current monitoring technique / Electroosmotic flow / Miniaturization / Nanochannels / Sacrificial layer technique DOI 10.1002/elps.200406083

1 Introduction

Nanofluidics can be defined as the study, description, and use of fluid flow around and inside nanoscale structures. The specific phenomena associated with fluid transport in nanosize channels is of considerable interest to achieve active control over the transport of specific molecular or ionic species. This may lead to enabling technologies by permitting new approaches to molecular separations and reactions in which one or more reagents are available in limited quantities [1]. In the past few years, fluidic channels with sub-μm height have been fabricated with conventional bulk and surface micromachining techniques [2–4]. So far, nanochannels have found application mainly in single molecule studies and molecular sieving [5–7] and in fundamental studies of the behavior of liquid in nanoconfinement [8].

The ability of manipulating liquids in nanochannels is crucial for these and future applications. Physical phenomena that become dominant with downscaling of dimensions can potentially be used as fluid handling mechanisms. Surface tension directed gas injection has been proven a suitable mechanism to move liquid in a channel of ~1 μm in height [9]. However, this method relies on the pneumatic actuation by a gas which would result in high external actuation pressures if applied to nanochannels, because of the high capillary counterpressure in these channels. In addition, nanochannels have a very high hydraulic resistance which leads to high actuation pressures for pneumatic pumping mechanisms in general. This complicates the implementation and the integration of nanochannels as part of an on-chip fluidic network. Electrokinetic actuation is an attractive alternative, as it is an on-chip pumping mechanism which requires only the integration of two contact electrodes. Besides, electroosmotic flow (EOF) has the advantage over pressure-driven flow that sample may be transported over long distances with less dispersion than pressure-driven flow due to the uniform plug-like velocity profile. These are the main reasons why EOF has become a widely used actuation mechanism for lab-on-a-chip [10–15].

In this paper, we present the results of our investigation to fabricate nanochannels, generate and measure electroosmotic flow in the nanochannels. The sacrificial layer technique [3] was used to fabricate channels with height in the order of 200 nm, and widths of few micrometers. The challenge in our study was to generate and measure low-volume flows, typically in the order of 0.1 pL/s in channels with a small cross-sectional area. These smallest generated flow rates are two orders of magnitude smaller than the resolution of the most sensitive existing flow sensors [16], and therefore the detection of the generated flows was one of the primary concerns. Initial calculations and measurements indicated that it is possible to measure the electrical resistance of nanochannels with an approximate cross-sectional area in the range of 0.1–1 μm^2 and a length of a few millimeters, filled by aqueous electrolyte solutions. We have therefore chosen to use a method based on the current monitoring technique [17] to measure the EOF-rate.

Correspondence: Dr. Petra Mela, MESA+ Institute for Nanotechnology, University of Twente, P.O. Box 217, NL-7500 AE Enschede, The Netherlands
E-mail: p.mela@el.utwente.nl
Fax: +31-53-489-3343

Abbreviations: CMOS, complementary metal oxide semiconductor; **MEMS**, microelectromechanical system

© 2004 WILEY-VCH Verlag GmbH & Co. KGaA, Weinheim

2 Materials and methods

2.1 Setup

The current monitoring technique [17] allows measuring EOF velocities independently of electrophoresis. It is based on the dependence of the fluid resistance on its ionic concentration. A channel (or capillary) is filled with an electrolyte solution of a certain ionic concentration, which is then replaced by the electroosmosis-driven flow of a second electrolyte solution with the same pH but different concentration. The overall resistance of the fluid in the channel will gradually change upon the replacement of one solution with the other and consequently the current in the channel will change. When the second solution has completely replaced the first one, the current reaches a constant value. By monitoring the current in time, it is therefore possible to monitor the flow in the channel (or capillary) and to calculate the average electroosmotic (EO) velocity. The length of the channel divided by the time needed for the complete replacement of the buffer is the EO velocity. The velocity divided by the applied electric field strength is the EO mobility. In our measurements, the EOF was induced by applying a voltage difference across the channel with a source-measurement unit (Keithley 2410 SourceMeter; Keithley Instruments, Cleveland, OH, USA) and platinum probes placed in the fluid reservoirs (Fig. 1a). The unit was interfaced to a computer *via* a GPIB-USB A (National Instruments, Austin, TX, USA) and controlled *via* a program written in HP VEE (Agilent Technologies, Palo Alto, CA, USA). The same source-measurement unit was used to monitor the current in time. Voltages and corresponding currents were recorded. In the Keithley SourceMeter the current is determined by the voltage drop across a measurement resistor (connected in series). To compensate for this voltage drop and to ensure a stable and constant output voltage, the SourceMeter has feedback control measur-

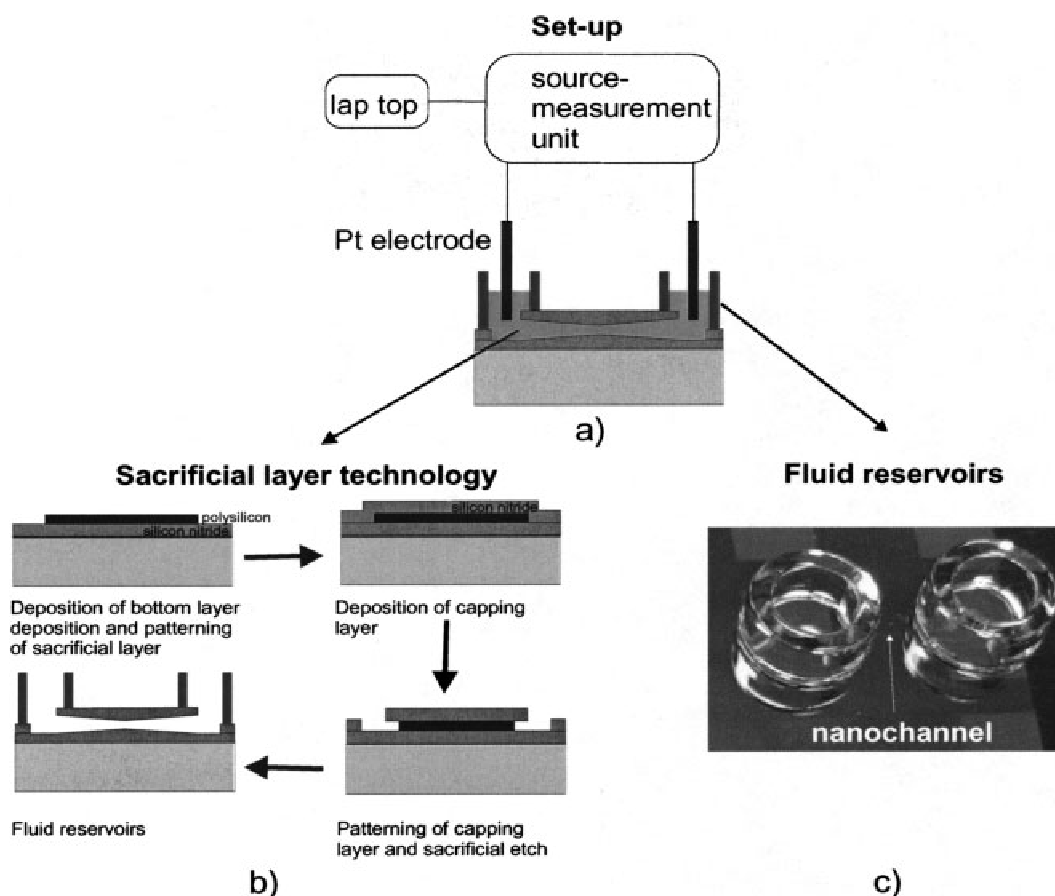

Figure 1. (a) Schematic representation of the experimental setup. (b) Fabrication process; polysilicon is used as sacrificial material, silicon nitride as capping layer and KOH as etchant. During the sacrificial etch, the openings of the channel are exposed longer to the KOH than the middle of the channel and the etching of the capping layer results in a tapered channel. (c) Picture of fluid reservoirs realized with glass rings.

© 2004 WILEY-VCH Verlag GmbH & Co. KGaA, Weinheim

ing the effective output voltage (after the current measurement resistor). The noise level in the current measurements was typically in the order of 30 pA, probably largely due to environmental causes as we used unshielded cables and probe set-up.

2.2 Preparation of the buffers

A 100 mM solution of L-histidine (HIS, p*K* = 6.0) and 2-(*N*-morpholino)ethanesulfonic acid (MES, p*K* = 6.15) was prepared. The pH of the solution was 6.1, the ionic concentration 53.1 mM (HIS^+, MES^-), and the conductivity 0.163 S/m. A 50 mM solution of HIS and MES was prepared upon dilution of the 100 mM. The pH of the 50 mM solution was 6.1, the concentration 26.0 mM, and the conductivity 0.09 S/m. The ionic concentrations of the buffers were calculated with the program PeakMaster*. The conductivity was measured using a commercial 4-point platinum conductivity probe (CDM210 Conductivity Meter; Radiometer Analytical S.A., Lyon, France). The buffer was chosen because of its low conductivity and its compatibility with biotechnology, cell biology, and molecular biology applications. The difference in the concentrations was chosen as to have a reasonably detectable difference in the currents obtained when the channels were filled with the different buffers. Because of the low conductivity, high concentrations can be used without generating significant Joule heating. In order to fix the pH at a certain level above the isoelectric point of the channel walls, a high concentration buffer is required in silica nanochannels, because the high surface-to-volume ratio results in a relative large amount of protons donated by the channel walls.

2.3 Channel fabrication

Nanochannels were created by sacrificial layer etching [3] on a 4-inch silicon wafer. The sacrificial layer technique is based on the use of a sacrificial layer patterned as the internal space of the channel, a capping layer that will form the walls of the channel, and a chemical etchant which will selectively etch the sacrificial material leaving the capping layer as structure on the wafer (b). The sacrificial layer technique can be complementary metal oxide semiconductor (CMOS)-compatible in terms of processing and materials. This means that the integration of electronics or microelectromechanical system (MEMS) structures is possible. However, other materials including polymeric materials can also be used. Other advantages of the technique are the possibility of integrating on-chip electrodes and the fact that no bonding steps are required to produce closed structures like fluidic channels. With this technique channels with very thin capping layers can be fabricated as required, for example, in near-field optical detection [18]. The main disadvantage for the fabrication of fluidic channels with this technique is that, despite the high selectivity of the etchant between sacrificial and capping material, during the sacrificial layer etching the channel walls are slightly etched as well. If the etch time required is long this will result in a tapered shape of the channel and a sufficiently thick capping layer will be needed. Furthermore, the etch rate of the sacrificial layer decreases with increasing etched channel length because of the slow diffusion of fresh etchant to the sacrificial material/etchant interface and the slow diffusion of by-products out of the channel [3].

The wafer was first oxidized to create a 1 μm thick SiO_2 insulating layer to prevent current flow through the wafer. A 0.4 μm thick silicon nitride layer was deposited by low-pressure chemical vapor deposition (LPCVD) to form the channel bottom layer. On top of that a 107 $\pm$ 3 nm thick sacrificial polysilicon layer was deposited by LPCVD and patterned by standard lithography and wet etching. These steps resulted in the formation of polysilicon lines representing the inside of the channels to be fabricated. In the mask design channels of 4 mm length and widths of 2, 4, and 8 μm were intended. The polysilicon lines were covered with 0.5 μm LPCVD silicon nitride to form the channel capping layer. After opening the capping layer at the two ends of the channel, the sacrificial polysilicon was etched in a 25 wt% KOH solution at 75°C for 96 h. The wafer was placed in water overnight to remove KOH from the channels by diffusion. Subsequently the wafer was placed in ethanol overnight so that the water could be replaced by ethanol. Finally, the channels were dried by spinning and baking the wafer at 120°C. Fluid reservoirs were created at the channel ends by placing glass rings (Schott-Duran) with a height of 2.5 mm and an inner diameter of 3.4 mm on the wafer and subsequently heating the wafer to 800°C for 30 min under nitrogen flow. Under these conditions, the glass slightly melts and adheres hermetically to the silicon nitride capping layer (Fig. 1c). After fabrication, the channels were inspected by optical microscopy to confirm that they were etched open. The effective channel widths were measured and resulted to be slightly different than the intended values: 1.7 $\pm$ 0.3 μm, 3.7 $\pm$ 0.3 μm, and 7.6 $\pm$ 0.3 μm, respectively.

* PeakMaster enables prediction of the behavior of background electrolytes in capillary zone electrophoresis. The mathematical background it uses is described in Gaš, B., Coufal, P., Jaros, M., Muzikar, J., Jelinek, I., *J. Chromatogr. A* 2001, *905*, 269–279, and in Stedry, M., Jaros, M., Gaš, B., *J. Chromatogr. A* 2002, *960*, 187–198.

© 2004 WILEY-VCH Verlag GmbH & Co. KGaA, Weinheim

Although the selectivity of the etchant between silicon nitride and polysilicon is rather high (1:10^5), during the sacrificial layer etching the silicon nitride channel walls were slightly etched as well. Since the openings of the channel were exposed longer to the KOH than the middle of the channel, the etching of the capping layer led to a total tapering in the channel height of 3.2 $\pm$ 0.9 nm per 100 μm channel length. The value of the tapering could be determined by analyzing atomic force microscopy (AFM) images taken on a 7.6 μm wide channel after the capping layer had been mechanically removed. Images were taken at different positions along the channel, and the change of the level of the channel bottom surface with respect to the (flat) silicon nitride surface surrounding the channel was used to determine the tapering. The images also showed that the surface of the device and the bottom of the exposed channels had not been damaged by the removing procedure. Based on this value for the tapering, the resulting channel height was estimated to increase from 145 $\pm$ 20 nm in the middle of the channel to 210 $\pm$ 40 nm at the openings.

2.4 Conditioning of the channels

Possible differences in surface properties can result in variations in EOF. The differences can be due to manufacturing or surface history and can be reduced by rinsing the channels with 0.1 M NaOH and deionized (DI) water. Initially, one of the reservoirs was filled with 0.1 M NaOH aqueous solution and the filling of the channel due to capillary forces was monitored under the objective of a top-down microscope to make sure no air bubbles were trapped. Freshly prepared channels filled without problems, while some days after fabrication they started to become contaminated and air bubbles were trapped inside the channels. Once the channel was filled, the other reservoir was also filled with the NaOH solution and a 19 V voltage difference was applied for 5 min between the two reservoirs. The same procedure was repeated with DI water and with 100 mM buffer. Every time the solutions were changed, the reservoirs were flushed three times and new pipette tips were used.

2.5 Experimental procedure

At the end of the conditioning procedure the channel was filled with high-concentration buffer (100 mM). One of the reservoirs was then filled with low-concentration buffer (50 mM) and a 19 V potential difference was applied over the channel to initiate EOF so that the lower concentration buffer could gradually fill the channel, replacing the higher concentration solution. The voltage was applied for 3 min during which current values were recorded. Subsequently, the other reservoir was filled with the higher concentration buffer and the voltage was applied again with inversed polarity. A set of ten measurements was obtained for channels with different widths. Examples of current/time traces for a channel approximately 7.6 μm wide are shown in Fig. 2. The time needed for the replacement of one buffer with the other was determined by the intersections of two horizontal lines and a straight line fitted with a least square method to the data points corresponding to a changing current (see Fig. 2). The horizontal lines correspond to the mean current values for the 100 mM buffer and for the 50 mM buffer. These values were determined by averaging all the data points of the corresponding plateau parts of the current/time traces, from the 75th second to the end of the trial (dotted window in Fig. 2). Current/time traces were obtained also with different voltages (10, 15, 40 V) to check for dependence of EO velocity on electric field.

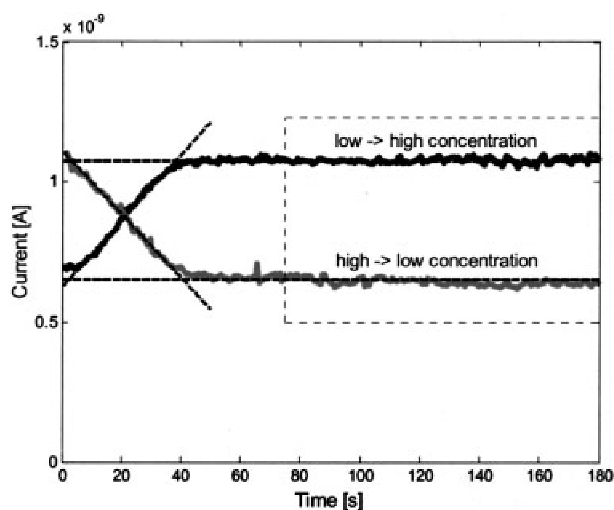

Figure 2. Examples of current-time traces obtained in a channel approximately 7.6 μm wide, 0.2 μm high, and 4 mm long when a voltage difference of 19 V was applied. When the lower-concentration buffer replaces the higher-concentration buffer, the current decreases as result of a higher resistance. The opposite is observed when the higher-concentration buffer replaces the lower-concentration buffer. The dotted rectangle delimits the time window in which mean current values were calculated. The horizontal lines correspond to mean current values.

3 Results and discussion

3.1 Current measurements

The measured current values are linearly dependent on channel width with a trend extending through the origin (Fig. 3). This is a strong indication that the measured

© 2004 WILEY-VCH Verlag GmbH & Co. KGaA, Weinheim

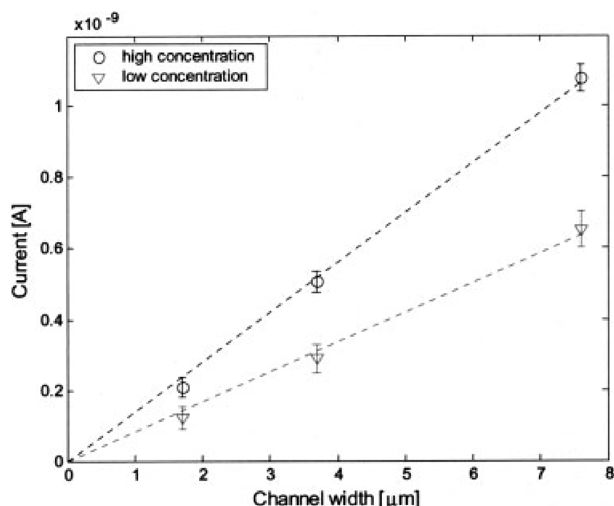

Figure 3. Mean current values ± 3 SD obtained for two different buffer concentrations in channels with different widths when a 19 V potential difference was applied along the channel.

currents are flowing inside the channels and excludes the possibility of occurrence of parasitic currents. Parasitic currents like currents over the surface of the wafer due to imperfect sealing of the reservoirs or leaking currents through the bulk silicon are not expected to scale with channel width. In a previous design the reservoirs consisted of droplets of buffer solution confined within hydrophobic barriers (fluorocarbon patterns deposited through a shadow mask). With this solution the measured currents exhibited large fluctuations and were not linearly dependent on channel width, most likely because of surface conduction over the silicon nitride capping layer.

The mean current values measured with the 100 mM buffer and the values measured with the 50 mM buffer are not in a 2:1 ratio, in accordance with the fact that the ratio between the bulk conductivities of the 100 mM and 50 mM buffers is not 2:1 because of an activity effect. The mobility of an ion decreases at increasing concentration because of interactions with ions with opposite charge. Hence, at high concentrations the bulk conductivity does not increase linearly with the number of ions. The electrophoretic resistance of the fluid is a function of its ionic concentration and can be evaluated from:

$$R_{ep} = \frac{l}{A \cdot q \cdot Na \cdot \sum_{i} (n_i \cdot \mu_i)} \tag{1}$$

where l and A are the length and the cross section of the channel, q is the elementary charge, Na is the Avogadro number, and n_i and μ_i are the concentration and the electrophoretic mobility of the charged species i. Writing for the conductivity of the solution $\kappa = q^*N_a^*\Sigma_i n_i\mu_i$, and taking into account the tapered shape of the channels when determining the resistance, Eq. (1) becomes:

$$R_{ep} = \frac{2 \cdot \log\left(\frac{h + \frac{t \cdot l}{2}}{h}\right)}{t \cdot w \cdot \kappa} \tag{2}$$

where h is the height in the middle of the channel, w the width of the channels, and t the tapering (3.2 nm/100 μm). By using this formula, the measured values are 95–115% of the expected values. The current values obtained at different voltages when the channels were filled with the 100 mM buffer are shown in Fig. 4. The dotted lines represent the current values expected on the base of the calculated R_{ep}.

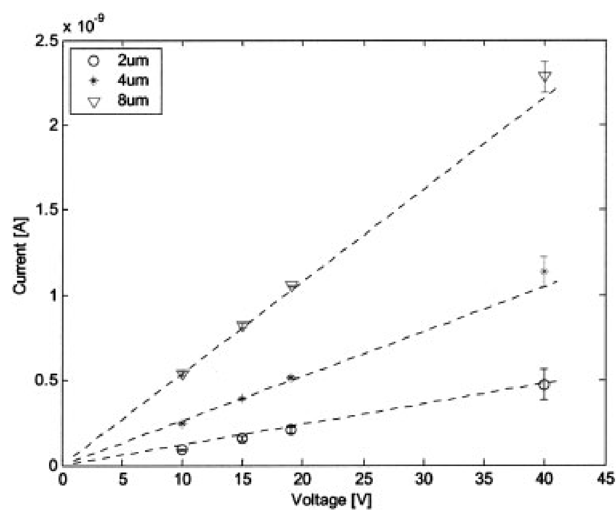

Figure 4. Measured data points and calculated (dotted lines) current as a function of applied voltage.

3.2 EOF measurements

To estimate EOF velocities, we focused on the measurements on the 7.6 μm wide channel as this provides the highest values of currents and therefore the highest level of accuracy. The mean EOF velocity determined from the ten current/time traces obtained at 19 V was 120±9 μm/s. The electroosmotic velocities as function of the applied voltage are plotted in Fig. 5. The data points for 19 V are determined on five trials each, while the other experimental points are obtained on a single trial. The data show a linear trend that indicates constant electroosmotic and electrophoretic mobilities and negligible temperature increases due to Joule heating. This is expected because of the small dimensions of the channels and the extremely low currents. Further evidence that the Joule heating can

© 2004 WILEY-VCH Verlag GmbH & Co. KGaA, Weinheim

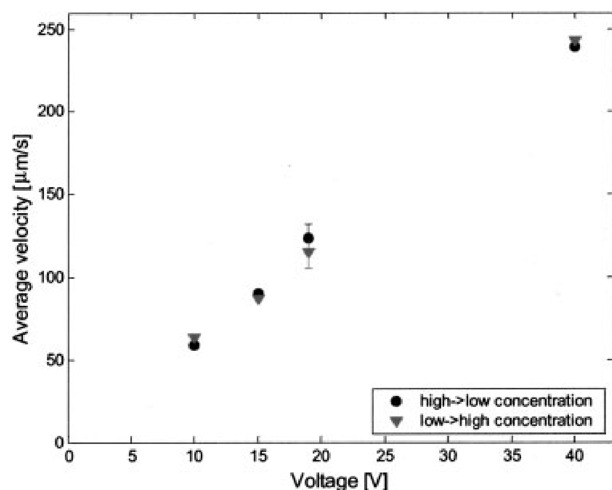

Figure 5. Electroosmotic velocity as a function of applied voltage in a 7.2 µm wide, 0.2 µm high, and 4 mm long channel. The velocity values for 19 V are mean values (n = 5) ± SD. Error bars are plotted for these values to give an indication of the accuracy of the measurements. All other data points were determined on a single measurement.

be neglected can be seen in the stability of the currents over a long period of time (approx. 3 min, Fig. 2) and for repeated measurements (Fig. 3). The velocities we calculated are in the range of 60–240 µm/s and correspond to average flow rates of 0.1–0.3 pL/s. The velocities we determined are mean velocities. In fact the flow field is not uniform along the channel as a consequence of the variations in the cross-sectional area, the nonuniform electric field and the changing buffer concentration along the channel. The flow we generated is therefore not purely electroosmotic, in fact a pressure gradient is induced in the channel to ensure constant flow rate in different sections [19].

From the velocities, a mean EO mobility (μ_{EO}) of $2.4 \times 10^{-8} m^2 V^{-1} s^{-1}$ is determined. The relation between zeta potential ξ and μ_{EO} is expressed by the Smoluchowski equation [20]:

$$\mu_{EO} = -\frac{\varepsilon \cdot \zeta}{\eta} \quad (3)$$

where ε and η are the permittivity and the viscosity of the medium, respectively. Assuming ε and η of water, an average ξ of -34 mV is obtained. Although this value is in good agreement with the zeta potential determined on silicon nitride thin films [15], it should be clear that it is a rough estimation. The zeta potential is in fact not uniform along the channels because of the significant difference in the two buffer concentrations we used.

4 Concluding remarks

We generated and monitored low-volume flows on-chip in channels with small cross-sectional area and height in the sub-µm range. Flow rates in the order of 0.1 pL/s were generated and successfully detected using the current monitoring method. Depending on the application of the device, close attention should be paid to the velocity profile. In nanochannels the thickness of the electric double layer (EDL) can represent a considerable part of the channel height, in which case the velocity profile of EOF cannot be considered flat anymore [21–23]. This is not the case in our experiments: due to the relative high buffer concentration, the double-layer thickness (approximately 2 nm) is small compared to the channel height, therefore, there is no double-layer overlap. However, because of the tapered shape of the channels and the large difference in the buffer concentrations, pressure is build up in the channels [19] and the flow profile is not flat.

An important application for ultralow-volume pumping is in fluidic interfacing to a single living cell. EO-pumping in thin-film fluidic channels is an important step towards truly integrated fluidic networks, which could find attractive application in high-speed combinatorial chemistry and chemical computing. The sacrificial layer technology offers the possibility of using a wide variety of materials, to be chosen according to the application's requirements (*e.g.*, optical transparency, low fluorescence background, chemical inertness, mechanical resistance, CMOS compatibility, monolithic integration of MEMS).

Received May 19, 2004

5 References

[1] Kuo, T.-C., Sloan, L. A., Sweedler, J. V., Bohn, P. W., *Langmuir* 2001, *17*, 6298–6303.

[2] Haneveld, J., Jansen, H. V., Berenschot, J. W., Tas, N. R., Elwenspoek, M. C., *J. Micromech. Microeng.* 2003, *13*, S62–S66.

[3] Stern, M. G., Geis, M. W., Curtin, J. E., *J. Vac. Sci. Technol. B* 1997, *15*, 2887–2891.

[4] Tas, N. R., Berenschot, J. W., Mela, P., Jansen, H. V., Elwenspoek, M., van den Berg, A., *Nano Lett.* 2002, *2*, 1031–1032.

[5] Foquet, M., Korlach, J., Zipfel, W., Webb, W. W., Craighead, H. G., *Anal. Chem.* 2002, *74*, 1415–1422.

[6] Han, J., Craighead, H. G., *Science* 2000, *288*, 1026–1029.

[7] Turner, S. W., Perez, A. M., Lopez, A., Craighead, H. G., *J. Vac. Sci. Technol. B* 1998, *16*, 3835–3840.

[8] Tas, N. R., Mela, P., Kramer, T., Berenschot, J. W., van den Berg, A., *Nano Lett.* 2003, *11*, 1537–1540.

[9] Tas, N. R., Berenschot, J. W., Lammerink, T. S. J., Elwenspoek, M., van den Berg, A., *Anal. Chem.* 2002, *74*, 2224–2227.

© 2004 WILEY-VCH Verlag GmbH & Co. KGaA, Weinheim

[10] Harrison, D. J., Manz, A., Fan, Z., Ludi, H., Widmer, H. M., *Anal. Chem.* 1992, *64*, 1926–1932.

[11] Harrison, D. J., Fluri, K., Seiler, K., Fan, Z. H., Effenhauser, C. S., Manz, A., *Science* 1993, *261*, 895–897.

[12] Jacobson, S. C., Hergenroder, R., Koutny, L. B., Ramsey, J. M., *Anal. Chem.* 1994, *66*, 1114–1118.

[13] Manz, A., Effenhauser, C. S., Burggraf, N., Harrison, D. J., Seiler, K., Fluri, K., *J. Micromech. Microeng.* 1994, *4*, 257–265.

[14] Schasfoort, R. B., Schlautmann, S., Hendrikse, J., van den Berg, A., *Science* 1999, *286*, 942–945.

[15] Bousse, L., Mostarshed, S., *J. Electroanal. Chem.* 1991, *302*, 269–274.

[16] Wu, S., Lin, Q., Yuen, Y., Tai, Y.-C., *Sens. Actuators A* 2001, *89*, 152–158.

[17] Huang, X., Gordon, M. J., Zare, R. N., *Anal. Chem.* 1988, *60*, 1837–1838.

[18] Li, W., Tegenfeldt, J. O., Chen, L., Austin, R. H., Chou, S. Y., Kohl, P. A., Krotine, J., Sturm, J. C., *Nanotechnology* 2003, *14*, 578–583.

[19] Ren, L., Escobedo, C., Li, D., *J. Colloid Interface Sci.* 2001, *242*, 264–271.

[20] Scales, P. J., Grieser, F., Healy, T. W., White, L. R., Chan, D. Y. C., *Langmuir* 1992, *8*, 965–974.

[21] Levine, S., Marriott, J. R., Robinson, K., *J. Chem. Soc. Farad. Trans. 2* 1975, *71*, 1–11.

[22] Jacobson, S. C., Alaire, J. P., Ramsey, J. M., *Proc. MicroTAS Conf.* 2001, 57–59.

[23] Ramsey, J. M., Alaire, J. P., S.C., J., Peterson, N. J., *Proc. MicroTAS Conf.* 2002, 314–316.

© 2004 WILEY-VCH Verlag GmbH & Co. KGaA, Weinheim